muscle because skeletal muscle development and function appears unaffected in miR-133a transgenic mice [59]. In this study, silencing of miR-133a had no toxic effect on muscle, including heart and skeletal muscle *in vivo* (**Supporting Information Fig. S7E–S7G**). Because the upregulation of miR-133a in osteosarcoma cells did not regulate the expression levels of CD133, we determined that it regulated multiple pathways that are not upstream of CD133 expression. Since the inducible factors of CD133 in osteosarcoma have not been cleared, further investigation of the relationship between the tumor microenvironment and CD133 might be warranted. Indeed, the activation of the hypoxia signaling pathway, for example, has been reported to trigger many pathways important for stem cell maintenance [60-62].

Second, we determined the efficacy of LNA technology, an antisense miRNA inhibitor oligonucleotide, as therapeutics against solid cancer. To date, the efficacy of LNAs against human disease has been reported in hepatitis and lymphoma. For example, LNA-anti-miR-122 (Miravirsen, Santaris Pharma, San Diego, CA) effectively treats chimpanzees infected with hepatitis C virus without any observable resistance or physiological side effects [63]. This treatment has advanced to phase 2 clinical trials, which emphasizes the strengths of anti-miR-122, including high efficacy and good tolerability without adverse effects [64]. The other report represents the preclinical trial of LNA-mediated miR-155 silencing against low-grade B-cell lymphoma [65]. Therefore, our preclinical study contributes to the broad application of LNA treatment including solid tumors. While an effective drug delivery system has been the most challenging remaining consideration for the successful translation of RNAi to the clinic for broad use in patients, the systemic administration of LNA-133a did not need assistance of drug delivery system to decrease the expression of miR-133a. These results are consistent with the results of the trial of LNA-anti-miR-122 against HCV infection, in which the LNA was injected via subcutaneous injection. This preclinical trial will not only provide a novel treatment strategy against osteosarcoma but will also support a wide range of LNA applications against cancers that require the silencing of specific miRNAs.

Third, the multiple targets of miR-133a were identified to have anti-tumor functions against osteosarcoma with clinical relevance. Using an

siRNA-induced gene knockdown system and a 3' UTR luciferase reporter assay, we identified sphingomyelin synthase 2 (*SGMS2*), ubiquitin-like modifier activating enzyme 2 (*UBA2*), sorting nexin family member 30 (*SNX30*), and annexin A2 (*ANXA2*) as novel anti-tumor molecules of osteosarcoma. Some of these molecules have been reported their association with other cancers but not for osteosarcoma. *SGMS2*, located on 4q25, is an enzyme that catalyzes the conversion of phosphatidylcholine and ceramide to sphingomyelin and diacylglycerol [66]. The specific activation of *SGMS2* explains the ability of this gene to trigger cell cycle arrest, cell differentiation, and autophagy or apoptosis in cancer cells [47]. *UBA2*, located on 19q12, forms a heterodimer that functions as a small ubiquitin-like modifier (SUMO)-activating enzyme for the sumoylation of proteins [67]. Conjugating SUMO-1, one of the four SUMO isoforms, to wild-type p53 increases the transactivation ability of p53 [45]. *SNX30*, located on 9q32, may mediate membrane association either through the lipid-binding PX domain (a phospholipid-binding motif) or protein-protein interactions. Although *SNX30* has not been well studied in cancer, loss of *SNX1*, one of the *SNX* families, plays a significant role in the development and aggressiveness of human colon cancer, at least partially through increased signaling from the endosomes [46]. In this study, we found correlations between the expression of *SGMS2*, *UBA2*, and *SNX30,* and osteosarcoma cell invasion, as well as a close correlation with the prognosis of osteosarcoma patients. *ANXA2*, located on 15q22, belongs to a large family of diverse proteins that are characterized by conserved annexin repeat domains and the ability to bind negatively charged phospholipids in a calcium-dependent manner [68]. The expression levels of *ANXA2* are decreased in a subset of human OS metastases and metastatic lines [69], but the actual role of *ANXA2* in suppressing OS metastasis has remained unclear [37], which was identified as a regulator of osteosarcoma cell invasion. In this study, we were unable to identify the target genes of miR-133a that were involved in cellular proliferation, which is a general characteristic of tumor-initiating cells. This result may provide one explanation for why the difference in the proliferation rate of the $CD133^{high}$ and $CD133^{low}$ cell populations was relatively small. Another reason for this difference may have been heterogeneiety even within the $CD133^{high}$ cell population. Further investigation of additional markers might shed

further light on the mechanisms underlying these phenotypes.

The most interesting and surprising results were the close correlations between the clinical behaviors of osteosarcoma and the expression of the factors associated with malignant tumor-initiating phenotypes, including CD133, miR-133a, and the target genes of miR-133a. These results support the importance of silencing of miR-133a during osteosarcoma treatment. Indeed, the target molecules of miR-133a were found to be significant and novel prognostic factors for osteosarcoma patients. Further analyses of these factors, including *SGMS2*, *UBA2*, and *SNX30,* would allow a better understanding of the molecular mechanisms that regulate osteosarcoma progression.

Overall, our study represents a novel approach for the use of RNAi therapeutics against the lethal phenotype of osteosarcoma. To the best of our knowledge, this study is the first preclinical trial of RNAi therapy overcoming the sarcoma malignancy. We found that miR-133a, which was induced by chemotherapy treatment, is a key regulator of cell invasion of the malignant cell population within osteosarcoma. In a pre-clinical *in vivo* experiment, systemic administration of LNA-133a with chemotherapy suppressed the osteosarcoma metastasis via the multiple pathways without any significant toxicity. Silencing of miR-133a may therefore represent a novel therapeutic strategy against osteosarcoma, which would lead to an improvement in the prognosis of osteosarcoma patients.

CONCLUSION

Silencing of miR-133a reduced the malignancy of $CD133^{high}$ osteosarcoma-initiating cell population through restoring the expression of multiple target genes. Systemic administration of LNA-antimiR-133a with cisplatin reduced lung metastasis and prolonged the survival of osteosarcoma-bearing mice. A clinical study revealed that high miR-133a expression levels within the patient biopsy specimens were significantly correlated with poor prognosis, providing the importance of regulating miR-133a levels in osteosarcoma for more efficient therapy in future.

ACKNOWLEDGMENTS

We gratefully thank T. Yamada for the cDNA library of osteosarcoma clinical samples. We also thank A. Inoue for her technical work. This work was supported in part by a grant-in-aid for the Third-Term Comprehensive 10-Year Strategy for Cancer Control of Japan, the Program for Promotion of Fundamental Studies in Health Sciences of the National Institute of Biomedical Innovation of Japan (NiBio), and a grant-in-aid for Scientific Research on Applying Health Technology from the Ministry of Health, Labour and Welfare of Japan.

Conflict of Interest

The authors have declared that no conflict of interest exists.

REFERENCES

1. Aogi K, Woodman A, Urquidi V, et al. Telomerase activity in soft-tissue and bone sarcomas. Clinical cancer research : an official journal of the American Association for Cancer Research. 2000;6:4776-4781.
2. Fletcher CD. The evolving classification of soft tissue tumours: an update based on the new WHO classification. Histopathology. 2006;48:3-12.
3. Naka N, Takenaka S, Araki N, et al. Synovial sarcoma is a stem cell malignancy. Stem Cells. 2010;28:1119-1131.
4. Reya T, Morrison SJ, Clarke MF, et al. Stem cells, cancer, and cancer stem cells. Nature. 2001;414:105-111.
5. Clarke MF, Dick JE, Dirks PB, et al. Cancer stem cells--perspectives on current status and future directions: AACR Workshop on cancer stem cells. Cancer research. 2006;66:9339-9344.
6. Clevers H. The cancer stem cell: premises, promises and challenges. Nature medicine. 2011;17:313-319.
7. Visvader JE, Lindeman GJ. Cancer stem cells in solid tumours: accumulating evidence and unresolved questions. Nature reviews. Cancer. 2008;8:755-768.
8. Allison DC, Carney SC, Ahlmann ER, et al. A meta-analysis of osteosarcoma outcomes in the modern medical era. Sarcoma. 2012;2012:704872.
9. Kawaguchi N, Ahmed AR, Matsumoto S, et al. The concept of curative margin in surgery for bone and soft tissue sarcoma. Clinical orthopaedics and related research. 2004:165-172.
10. Gupta A, Meswania J, Pollock R, et al. Non-invasive distal femoral expandable endoprosthesis for limb-salvage surgery in paediatric tumours. The

Journal of bone and joint surgery. British volume. 2006;88:649-654.

11. Bacci G, Rocca M, Salone M, et al. High grade osteosarcoma of the extremities with lung metastases at presentation: treatment with neoadjuvant chemotherapy and simultaneous resection of primary and metastatic lesions. Journal of surgical oncology. 2008;98:415-420.
12. Halldorsson A, Brooks S, Montgomery S, et al. Lung metastasis 21 years after initial diagnosis of osteosarcoma: a case report. Journal of medical case reports. 2009;3:9298.
13. Adhikari AS, Agarwal N, Wood BM, et al. CD117 and Stro-1 identify osteosarcoma tumor-initiating cells associated with metastasis and drug resistance. Cancer research. 2010;70:4602-4612.
14. Basu-Roy U, Seo E, Ramanathapuram L, et al. Sox2 maintains self renewal of tumor-initiating cells in osteosarcomas. Oncogene. 2012;31:2270-2282.
15. Gibbs CP, Kukekov VG, Reith JD, et al. Stem-Like Cells in Bone Sarcomas: Implications for Tumorigenesis. Neoplasia. 2005;7:967-976.
16. Levings PP, McGarry SV, Currie TP, et al. Expression of an exogenous human Oct-4 promoter identifies tumor-initiating cells in osteosarcoma. Cancer research. 2009;69:5648-5655.
17. Siclari VA, Qin L. Targeting the osteosarcoma cancer stem cell. Journal of orthopaedic surgery and research. 2010;5:78.
18. Tirino V, Desiderio V, d'Aquino R, et al. Detection and characterization of CD133+ cancer stem cells in human solid tumours. PloS one. 2008;3:e3469.
19. Tirino V, Desiderio V, Paino F, et al. Human primary bone sarcomas contain CD133+ cancer stem cells displaying high tumorigenicity in vivo. FASEB journal : official publication of the Federation of American Societies for Experimental Biology. 2011;25:2022-2030.
20. Wilson H, Huelsmeyer M, Chun R, et al. Isolation and characterisation of cancer stem cells from canine osteosarcoma. Vet J. 2008;175:69-75.
21. Wu C, Wei Q, Utomo V, et al. Side population cells isolated from mesenchymal neoplasms have tumor initiating potential. Cancer research. 2007;67:8216-8222.
22. Gregory RI, Shiekhattar R. MicroRNA biogenesis and cancer. Cancer research. 2005;65:3509-3512.
23. Ambros V. microRNAs: tiny regulators with great potential. Cell. 2001;107:823-826.
24. Calin GA, Croce CM. MicroRNA signatures in human cancers. Nature reviews. Cancer. 2006;6:857-866.
25. Esquela-Kerscher A, Slack FJ. Oncomirs - microRNAs with a role in cancer. Nature reviews. Cancer. 2006;6:259-269.
26. Ma S, Tang KH, Chan YP, et al. miR-130b Promotes CD133(+) liver tumor-initiating cell growth and self-renewal via tumor protein 53-induced nuclear protein 1. Cell stem cell. 2010;7:694-707.

27. Calin GA, Ferracin M, Cimmino A, et al. A MicroRNA signature associated with prognosis and progression in chronic lymphocytic leukemia. The New England journal of medicine. 2005;353:1793-1801.

28. Jiang J, Gusev Y, Aderca I, et al. Association of MicroRNA expression in hepatocellular carcinomas with hepatitis infection, cirrhosis, and patient survival. Clinical cancer research : an official journal of the American Association for Cancer Research. 2008;14:419-427.

29. Kawai A, Ozaki T, Ikeda S, et al. Two distinct cell lines derived from a human osteosarcoma. Journal of cancer research and clinical oncology. 1989;115:531-536.

30. Osaki M, Takeshita F, Sugimoto Y, et al. MicroRNA-143 regulates human osteosarcoma metastasis by regulating matrix metalloprotease-13 expression. Molecular Therapy. 2011;19:1123-1130.

31. Youden W. Index for rating diagnostic tests. Cancer. 1950;3:32-35.

32. Gires O. Lessons from common markers of tumor-initiating cells in solid cancers. Cellular and molecular life sciences : CMLS. 2011;68:4009-4022.

33. Cao Y, Zhou Z, de Crombrugghe B, et al. Osterix, a transcription factor for osteoblast differentiation, mediates antitumor activity in murine osteosarcoma. Cancer research. 2005;65:1124-1128.

34. de Crombrugghe B, Lefebvre V, Behringer RR, et al. Transcriptional mechanisms of chondrocyte differentiation. Matrix Biology. 2000;19:389-394.

35. Ducy P, Zhang R, Geoffroy V, et al. Osf2/Cbfa1: a transcriptional activator of osteoblast differentiation. Cell. 1997;89:747-754.

36. Nakashima K, Zhou X, Kunkel G, et al. The novel zinc finger-containing transcription factor osterix is required for osteoblast differentiation and bone formation. Cell. 2002;108:17-29.

37. Tang N, Song WX, Luo J, et al. Osteosarcoma development and stem cell differentiation. Clinical orthopaedics and related research. 2008;466:2114-2130.

38. Croce CM. Causes and consequences of microRNA dysregulation in cancer. Nature reviews. Genetics. 2009;10:704-714.

39. Elmen J, Lindow M, Schutz S, et al. LNA-mediated microRNA silencing in non-human primates. Nature. 2008;452:896-899.

40. Haraguchi T, Nakano H, Tagawa T, et al. A potent 2'-O-methylated RNA-based microRNA inhibitor with unique secondary structures. Nucleic acids research. 2012;40:e58.

41. Obad S, dos Santos CO, Petri A, et al. Silencing of microRNA families by seed-targeting tiny LNAs. Nature genetics. 2011;43:371-378.

42. Dass CR, Ek ET, Choong PF. Human xenograft osteosarcoma models with spontaneous metastasis in

mice: clinical relevance and applicability for drug testing. J Cancer Res Clin Oncol. 2007;133:193-198.

43. Kimura K, Nakano T, Park Y-B, et al. Establishment of human osteosarcoma cell lines with high metastatic potential to lungs and their utilities for therapeutic studies on metastatic osteosarcoma. Clinical & experimental metastasis. 2002;19:477-486.
44. Tsuchida R, Das B, Yeger H, et al. Cisplatin treatment increases survival and expansion of a highly tumorigenic side-population fraction by upregulating VEGF/Flt1 autocrine signaling. Oncogene. 2008;27:3923-3934.
45. Gostissa M, Hengstermann A, Fogal V, et al. Activation of p53 by conjugation to the ubiquitin-like protein SUMO-1. The EMBO journal. 1999;18:6462-6471.
46. Nguyen LN, Holdren MS, Nguyen AP, et al. Sorting nexin 1 down-regulation promotes colon tumorigenesis. Clinical cancer research : an official journal of the American Association for Cancer Research. 2006;12:6952-6959.
47. Ségui B, Andrieu-Abadie N, Jaffrézou J-P, et al. Sphingolipids as modulators of cancer cell death: potential therapeutic targets. Biochimica et Biophysica Acta (BBA)-Biomembranes. 2006;1758:2104-2120.
48. Gillette JM, Chan DC, Nielsen-Preiss SM. Annexin 2 expression is reduced in human osteosarcoma metastases. Journal of cellular biochemistry. 2004;92:820-832.
49. Shackleton M, Quintana E, Fearon ER, et al. Heterogeneity in cancer: cancer stem cells versus clonal evolution. Cell. 2009;138:822-829.
50. Yin AH, Miraglia S, Zanjani ED, et al. AC133, a novel marker for human hematopoietic stem and progenitor cells. Blood. 1997;90:5002-5012.
51. Marzesco AM, Janich P, Wilsch-Brauninger M, et al. Release of extracellular membrane particles carrying the stem cell marker prominin-1 (CD133) from neural progenitors and other epithelial cells. Journal of cell science. 2005;118:2849-2858.
52. Uchida N, Buck DW, He D, et al. Direct isolation of human central nervous system stem cells. Proceedings of the National Academy of Sciences of the United States of America. 2000;97:14720-14725.
53. Freund D, Bauer N, Boxberger S, et al. Polarization of human hematopoietic progenitors during contact with multipotent mesenchymal stromal cells: effects on proliferation and clonogenicity. Stem cells and development. 2006;15:815-829.
54. Ma L, Reinhardt F, Pan E, et al. Therapeutic silencing of miR-10b inhibits metastasis in a mouse mammary tumor model. Nature biotechnology. 2010;28:341-347.
55. Ma L, Teruya-Feldstein J, Weinberg RA. Tumour invasion and metastasis initiated by microRNA-10b in breast cancer. Nature. 2007;449:682-688.

56. Preis M, Gardner TB, Gordon SR, et al. MicroRNA-10b expression correlates with response to neoadjuvant therapy and survival in pancreatic ductal adenocarcinoma. Clinical cancer research : an official journal of the American Association for Cancer Research. 2011;17:5812-5821.

57. Gabriely G, Yi M, Narayan RS, et al. Human glioma growth is controlled by microRNA-10b. Cancer research. 2011;71:3563-3572.

58. Chen JF, Mandel EM, Thomson JM, et al. The role of microRNA-1 and microRNA-133 in skeletal muscle proliferation and differentiation. Nature genetics. 2006;38:228-233.

59. Deng Z, Chen JF, Wang DZ. Transgenic overexpression of miR-133a in skeletal muscle. BMC musculoskeletal disorders. 2011;12:115.

60. Heddleston JM, Li Z, Lathia JD, et al. Hypoxia inducible factors in cancer stem cells. British journal of cancer. 2010;102:789-795.

61. Iida H, Suzuki M, Goitsuka R, et al. Hypoxia induces CD133 expression in human lung cancer cells by up-regulation of OCT3/4 and SOX2. Int J Oncol. 2012;40:71-79.

62. Soeda A, Park M, Lee D, et al. Hypoxia promotes expansion of the CD133-positive glioma stem cells through activation of HIF-1alpha. Oncogene. 2009;28:3949-3959.

63. Lanford RE, Hildebrandt-Eriksen ES, Petri A, et al. Therapeutic silencing of microRNA-122 in primates with chronic hepatitis C virus infection. Science. 2010;327:198-201.

64. Kim M, Kasinski AL, Slack FJ. MicroRNA therapeutics in preclinical cancer models. Lancet Oncol. 2011;12:319-321.

65. Zhang Y, Roccaro AM, Rombaoa C, et al. LNA-mediated anti-miR-155 silencing in low-grade B-cell lymphomas. Blood. 2012;120:1678-1686.

66. Huitema K, van den Dikkenberg J, Brouwers JFHM, et al. Identification of a family of animal sphingomyelin synthases. The EMBO journal. 2004;23:33-44.

67. Hay RT. SUMO: a history of modification. Molecular cell. 2005;18:1-12.

68. Balch C, Dedman JR. Annexins II and V inhibit cell migration. Experimental cell research. 1997;237:259-263.

69. Mintz MB, Sowers R, Brown KM, et al. An expression signature classifies chemotherapy-resistant pediatric osteosarcoma. Cancer research. 2005;65:1748-1754.

See www.StemCells.com for supporting information available online.

Figure 1. The phenotypic differences and clinical relevance based on the expression of CD133 in osteosarcoma cells. (**A**) The frequency of $CD133^{high}$ cell populations in SaOS2 osteosarcoma cell lines based on FACS analysis. See also **Supporting Information Figure S1A**. (**B,C**) Sphere-formation assays using freshly isolated $CD133^{high}$ and $CD133^{low}$ SaOS2 cells. The images were captured on day 10 (**B**) and the ratios of the wells containing spheres (middle) formed from single cells (top) were counted (**C**). The wells containing the cells that did not form spheres (bottom) were excluded. Scale bar, 50 μm. Data are presented as mean ± s.d. (n = 4 per group). *p <0.05; Student's t test. (**D**) Drug sensitivity of $CD133^{high}$ and $CD133^{low}$ SaOS2 cells. Cell viability after doxorubicin (DOX, 0.18 μM), cisplatin (CDDP, 2.5 μM), or methotrexate (MTX, 0.08 μM) treatment was analyzed. Data are presented as mean ± s.d. (n = 3 per group). *$p < 0.05$; Student's t test. (**E,F**) Invasion assays in $CD133^{high}$ and $CD133^{low}$ SaOS2 cell populations (n = 3 per group). The number of invaded cell were photographed (**E**) and counted (**F**). Data are presented as mean ± s.d. (n = 3 per group). ** $p < 0.01$; Student's t test. Scale bar, 200 μm. (**G**) qPCR analysis of stem cell-associated, multiple drug-resistant transporters, and metastasis-associated genes of $CD133^{high}$ and $CD133^{low}$ SaOS2 cell populations. β-actin was uses as an internal control. Data are presented as mean ± s.d. (n = 3 per group). (**H**) Limiting dilution analysis of $CD133^{high}$ (red circles) and $CD133^{low}$ (green circles) SaOS2-luc cell populations *in vivo*. Both cell populations were injected orthotopically into mice (n = 4 per group). The upper figure represents the tumor formation in mice from 1×10^3 cells of $CD133^{high}$ cells. The lower table shows the number of mice that developed tumors from various numbers of $CD133^{high}$ or $CD133^{low}$ cells. The tumor growth from $CD133^{high}$ cells was observed in 0/4 mice at 10^2 cells, 3/4 mice at 10^3 cells, 4/4 mice at 10^4 cells, and 4/4 mice at 10^5 cells, while those from $CD133^{low}$ cells was observed in 0/4 mice at 10^2 cells, 1/4 mice at 10^3 cells, 4/4 mice at 10^4 cells, and 4/4 mice at 10^5 cells. (**I,J**) The Kaplan-Meier curves for overall survival (**I**; $p = 0.026$; log-rank test) and disease-free survival (**J**; $p = 0.065$, log-rank test) based on the level of CD133 expression in the biopsy specimens from 35 osteosarcoma patients. See also **Supporting Information Figure S2A and Table S1**.

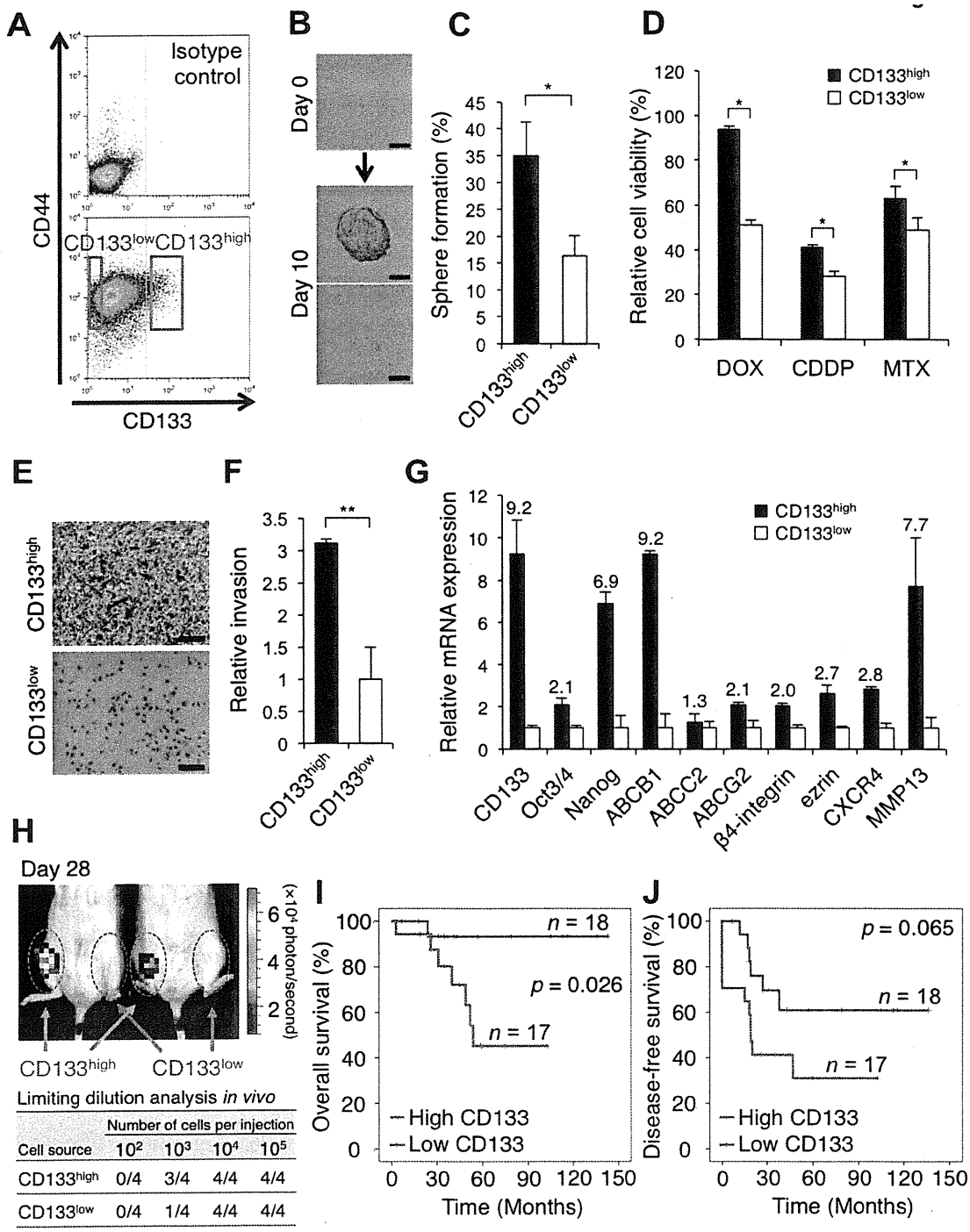
A
Isotype control
CD44
CD133low CD133high
CD133
B
Day 0
Day 10
C
Sphere formation (%)
CD133high
CD133low
D
Relative cell viability (%)
CD133high
CD133low
DOX
CDDP
MTX
E
CD133high
CD133low
F
Relative invasion
CD133high
CD133low
G
Relative mRNA expression
CD133high
CD133low
9.2
2.1
6.9
9.2
1.3
2.1
2.0
2.7
2.8
7.7
CD133
Oct3/4
Nanog
ABCB1
ABCC2
ABCG2
β4-integrin
ezrin
CXCR4
MMP13
H
Day 28
(×10⁶ photon/second)
CD133high
CD133low
Limiting dilution analysis in vivo
Number of cells per injection
Cell source 10² 10³ 10⁴ 10⁵
CD133high 0/4 3/4 4/4 4/4
CD133low 0/4 1/4 4/4 4/4
I
Overall survival (%)
n = 18
p = 0.026
n = 17
High CD133
Low CD133
Time (Months)
J
Disease-free survival (%)
p = 0.065
n = 18
n = 17
High CD133
Low CD133
Time (Months)

Figure 2. miR-133a regulates cell invasion of TIC cell population within osteosarcoma and represents prognostic value. (**A**) The upregulated expression levels of miR-1, 10b, and 133a in $CD133^{high}$ cell population. Data are presented as mean ± s.d. ($n = 3$ per group). *$p < 0.05$, **$p < 0.01$, ***$p < 0.001$; Student's t test. (**B,C**) Invasion assays in purified $CD133^{low}$ SaOS2 cells transfected with miR-1, 10b, and 133a oligos. $CD133^{low}$ SaOS2 cell populations were transfected with miR-1, 10b, 133a, or NC mimics at a final concentration of 30 nM. At the time periods of 24 h post-transfection, cells were seeded and cultured on the invasion chamber for 36 h. The number of invaded cell were photographed (**B**) and counted (**C**). Scale bar, 200 μm. Data are presented as mean ± s.d. ($n = 3$ per group). **$p < 0.01$, ***$p < 0.001$, calculated with one-way ANOVA with Bonferroni's multiple comparison when compared with the $CD133^{low}$ cell population treated with miR-NC. (**D**) The expression level of miR-133a in $CD133^{high}$ and $CD133^{low}$ populations of freshly resected patient biopsies. (**E,F**) The Kaplan-Meier curves for overall survival (**E**) and disease-free survival (**F**) based on the levels of miR-133a expression in 48 formalin-fixed paraffin-embedded (FFPE) tissues from osteosarcoma biopsy specimens, as determined using qRT-PCR. The overall survival rate ($p = 0.032$; log-rank test) and disease-free survival rate ($p = 0.081$; log-rank test) for osteosarcoma patients with high miR-133a expression (red line) were compared with those for patients with low miR-133a expression (green line). See also **Supporting Information Figure S2B** and Table S2. (G,H) Invasion assays in LNA-133a-treated SaOS2 $CD133^{high}$ populations. $CD133^{high}$ and $CD133^{low}$ SaOS2 cell populations were isolated and transfected with LNA-133a or LNA-NC to reduce the expression of miR-133a in the $CD133^{high}$ cell population. As a control, $CD133^{low}$ cell populations were transfected with LNA-NC. At the time periods of 24 h post-transfection, cells were seeded and cultured on the invasion chamber for 36 h. The number of invaded cell were photographed (**G**) and counted (**H**). Scale bar, 200 μm. Data are presented as mean ± s.d. ($n = 3$ per group). ***$p < 0.001$, calculated with one-way ANOVA with Bonferroni's multiple comparison when compared with the $CD133^{high}$ cell populations treated with LNA-NC.

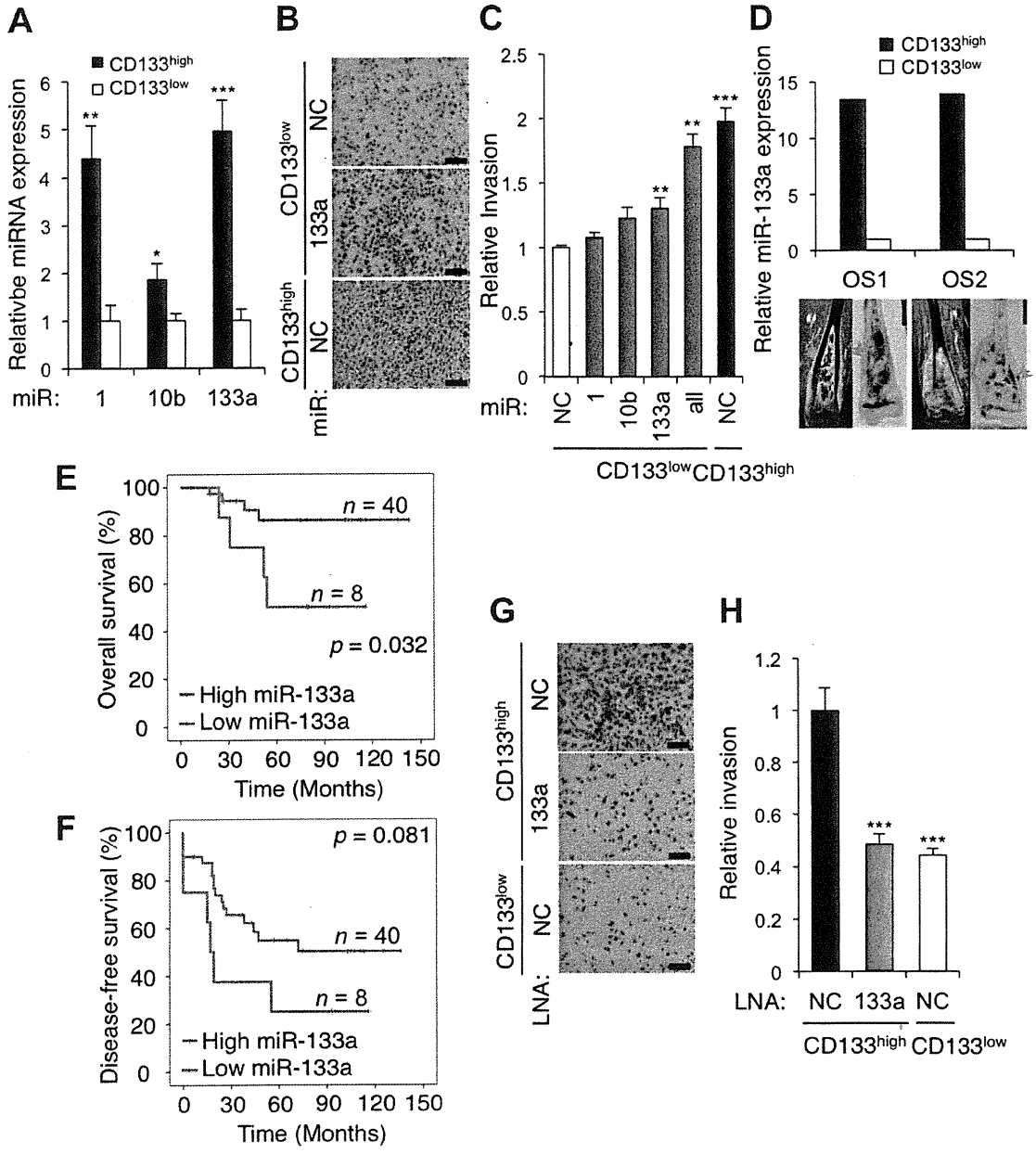
A
CD133high
CD133low
Relativbe miRNA expression
miR: 1 10b 133a
B
CD133low
CD133high
NC
133a
miR:
C
Relative Invasion
miR: NC 1 10b 133a all NC
CD133lowCD133high
D
CD133high
CD133low
Relative miR-133a expression
OS1
OS2
E
Overall survival (%)
n = 40
n = 8
p = 0.032
High miR-133a
Low miR-133a
Time (Months)
F
Disease-free survival (%)
p = 0.081
n = 40
n = 8
High miR-133a
Low miR-133a
Time (Months)
G
CD133high
CD133low
NC
133a
LNA:
H
Relative invasion
LNA: NC 133a NC
CD133high CD133low

Figure 3. Chemotherapy induces the expression of miR-133a in highly malignant osteosarcoma 143B cells. (**A**,**B**) Invasion assay in highly metastatic osteosarcoma 143B cells treated with LNA-133a and NC. At the time periods of 24 h post-transfection, cells were seeded and cultured on the invasion chamber for 24 h. The number of invaded cell were photographed (**A**) and counted (**B**). Scale bar, 200 μm. Data are presented as mean ± s.d. (n = 3 per group). *p < 0.05; Student's t test. (**C**) The induced expression of CD133 in 143B cells in the presence of chemotherapeutics (DOX and CDDP, 48 h). Data are presented as mean ± s.d. (n = 3 per group). **p < 0.01, ***p < 0.001, calculated with one-way ANOVA with Bonferroni's multiple comparison when compared with untreated cells. (**D**) The induced expression of miR-133a in 143B cells in the presence of chemotherapeutics (DOX and CDDP, 48 h). Data are presented as mean ± s.d. (n = 3 per group). ***p < 0.001, calculated with one-way ANOVA with Bonferroni's multiple comparison when compared with untreated cells.

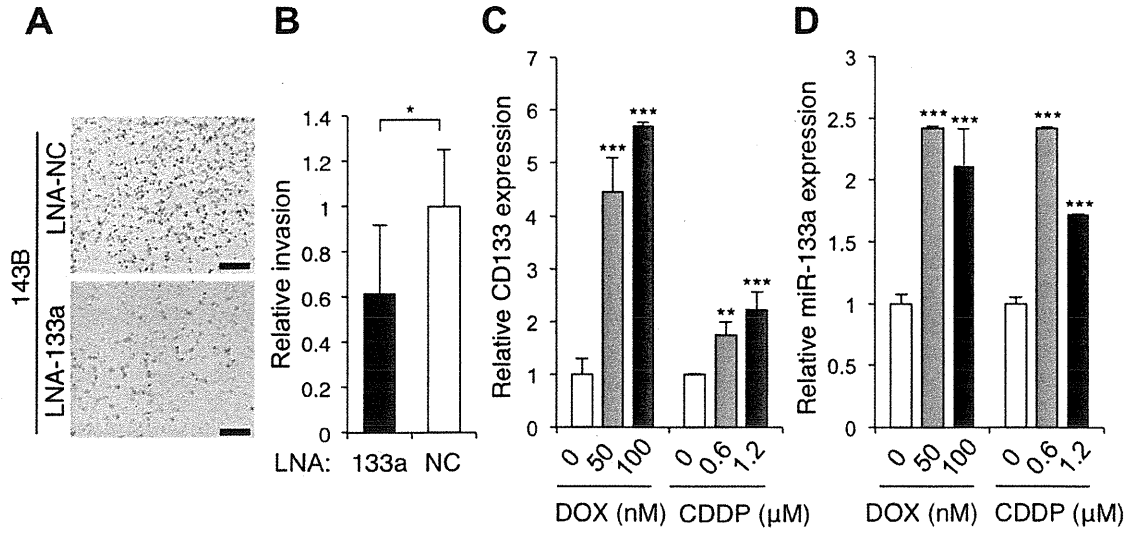

Figure 4. Therapeutic administration of LNA-anti-miR-133a with systemic chemotherapy inhibits osteosarcoma progression *in vivo*. (A) A schematic representation of the LNA-133a (red arrow) and cisplatin (blue arrow) administration schedule for 143B-luc-bearing mice. (**B**) The expression levels of miR-133a in osteosarcoma tissues (n = 5 per group) analyzed by qRT-PCR. The tumors were obtained during autopsy after completion of treatment on day 22. Data are presented as mean ± s.d. (n = 5 per group). $^{**}p < 0.01$, as compared to control saline-treated group; Student's t test. (**C,D**) Tumors at the primary site of each treatment group measured on day 22. The macroscopic appearances of 143B-luc tumors in each group of mice on day 22 are shown (**C**). The tumor masses outlined by a dotted line. Scale bar, 10 mm. The 143B-luc tumors from each group of mice were weighed on day 22 (**D**). Data are presented as mean ± s.d. (n = 5 per group). $^{*}p < 0.05$, as compared to control saline-treated group; Student's t test. (**E** to **G**) The lung metastases of each treatment group measured on day 22 using an *in vivo* imaging system (IVIS). The representative luminescence of the chest lesions in each group of mice was determined (**E**). For each mouse that was sacrificed to validate the lung metastases, each lung was re-evaluated using IVIS (**F**). The representative average luminescence of the chest region in each group of mice (n = 10) was compared among the treatment groups (**G**). Data are presented as mean ± s.d. (n = 5 per group). $^{*}p < 0.05$, as compared with LNA-NC/CDDP and LNA-133a/CDDP group; Student's t test. (**H**) Lung metastases validated by H&E staining. Black arrow represents metastatic foci in the lung. Scale bars, 500 μm. (**I**) Survival curves for each group of mice by Kaplan-Meier analysis. Log-rank test was performed between LNA-NC/CDDP group (blue line) and LNA-133a/CDDP group (red line) ($^{*}p = 0.026$).

Figure 4

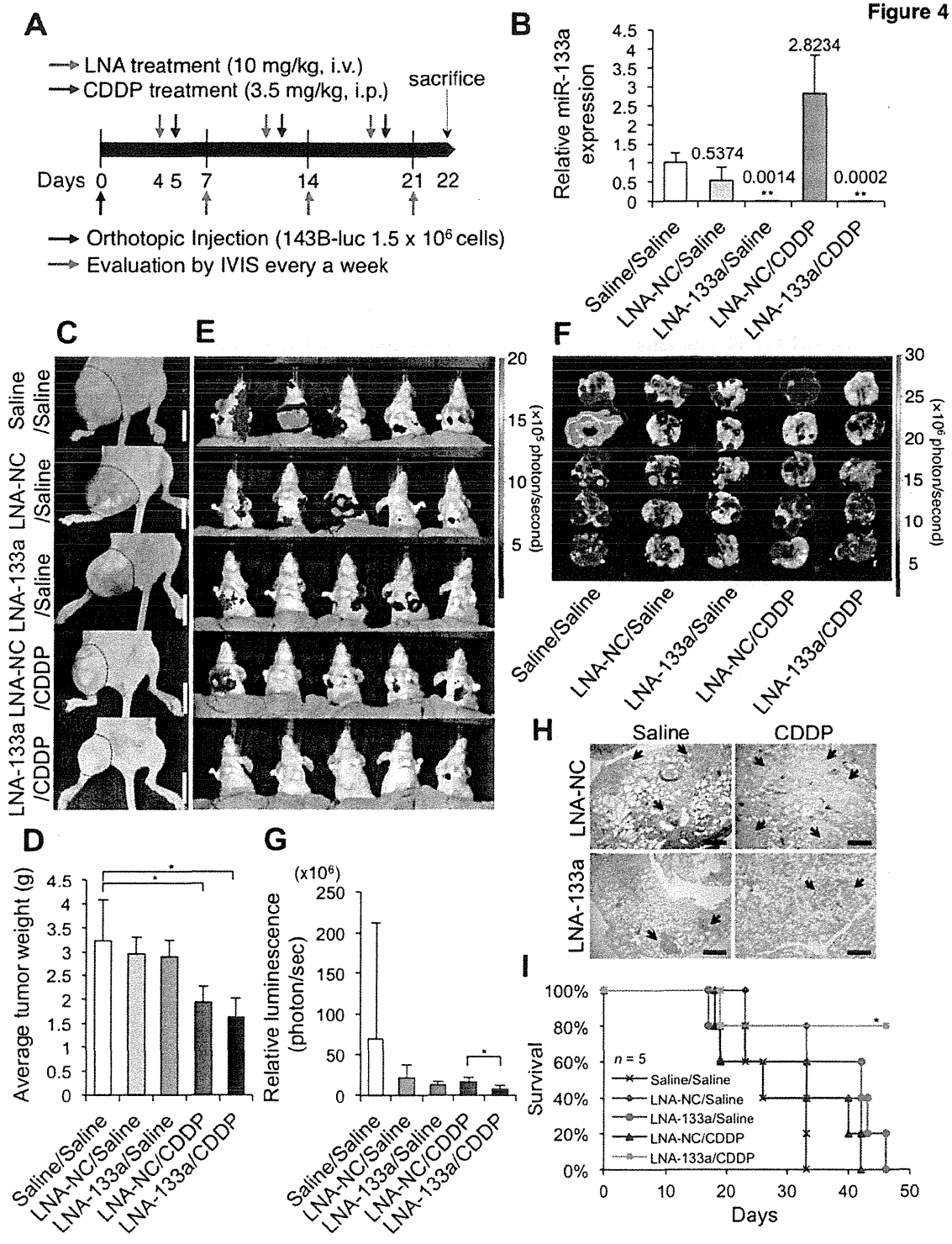
A
LNA treatment (10 mg/kg, i.v.)
CDDP treatment (3.5 mg/kg, i.p.)
sacrifice
Days 0 4 5 7 14 21 22
Orthotopic Injection (143B-luc 1.5 x 10^6 cells)
Evaluation by IVIS every a week
B
Relative miR-133a expression
0.5374
0.0014
2.8234
0.0002
Saline/Saline
LNA-NC/Saline
LNA-133a/Saline
LNA-NC/CDDP
LNA-133a/CDDP
C
E
F
Saline /Saline
LNA-NC /Saline
LNA-133a /Saline
LNA-NC /CDDP
LNA-133a /CDDP
(x10^5 photon/second)
(x10^6 photon/second)
D
Average tumor weight (g)
G
(x10^6)
Relative luminescence (photon/sec)
H
Saline
CDDP
LNA-NC
LNA-133a
I
Survival
n = 5
Saline/Saline
LNA-NC/Saline
LNA-133a/Saline
LNA-NC/CDDP
LNA-133a/CDDP
Days

Figure 5. The direct target genes of miR-133a regulate malignant phenotypes of osteosarcoma. (**A**) A Venn diagram of the candidate target mRNAs of miR-133a based on the cDNA microarrays and *in silico* database. (**B**) Invasion assays performed using SaOS2 cells 24 h post-transfection of the 10 siRNAs. $CD133^{high}$ and $CD133^{low}$ SaOS2 cell populations were isolated using flow cytometry and transfected with 10 siRNAs against the identified genes in (**A**). Data are presented as mean ± s.d. ($n = 3$ per group). $*p < 0.05$, $**p < 0.01$, $***p < 0.001$, calculated with one-way ANOVA with Bonferroni's multiple comparison when compared with the $CD133^{low}$ cells transfected with non-targeting siRNA. (**C**) Schematics of the miR-133a binding site within the 3' UTR of the target mRNAs. (D) Luciferase activities measured by co-transfecting miR-133a oligos and the luciferase reporters. Data are presented as mean ± s.d. ($n = 3$ per group). $*p < 0.05$, $**p < 0.01$; Student's t test. (**E** and **F**) Representative SGMS2 immunohistochemistry images of 143B-luc tumor sections (**E**) and the relative SGMS2 expression of 143B-luc tumor sections performed by qRT-PCR analysis (**F**). Scale bars, 50 μm. Data are presented as mean ± s.d. ($n = 3$ per group). $**p < 0.01$; Student's t test.

Figure 5

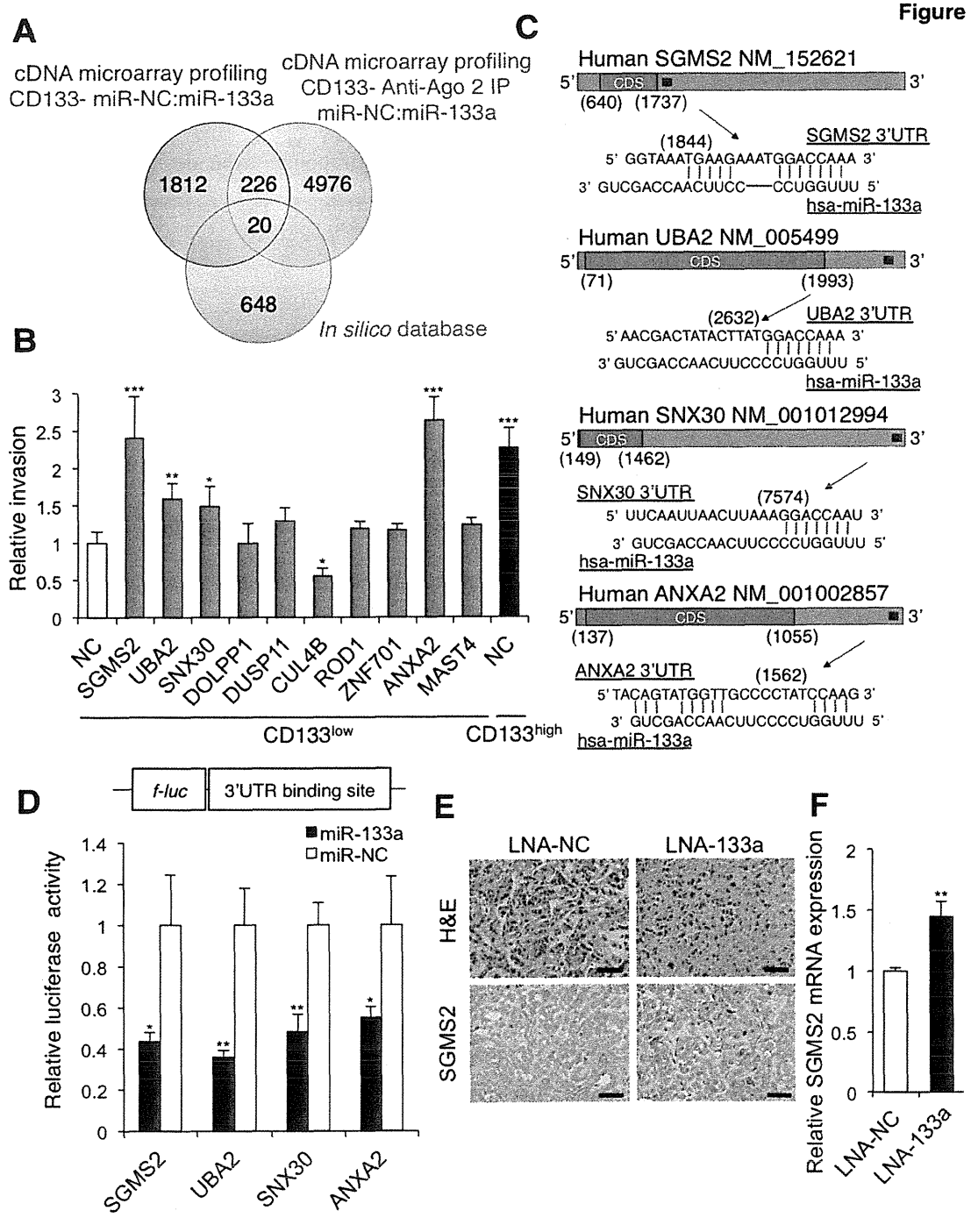
A
cDNA microarray profiling
CD133- miR-NC:miR-133a
cDNA microarray profiling
CD133- Anti-Ago 2 IP
miR-NC:miR-133a
1812
226
4976
20
648
In silico database
B
Relative invasion
NC
SGMS2
UBA2
SNX30
DOLPP1
DUSP11
CUL4B
ROD1
ZNF701
ANXA2
MAST4
NC
CD133low
CD133high
C
Human SGMS2 NM_152621
CDS
(640) (1737)
(1844)
SGMS2 3'UTR
5' GGTAAATGAAGAAATGGACCAAA 3'
3' GUCGACCAACUUCC—CCUGGUUU 5'
hsa-miR-133a
Human UBA2 NM_005499
(71)
(1993)
(2632)
UBA2 3'UTR
5' AACGACTATACTTATGGACCAAA 3'
3' GUCGACCAACUUCCCCUGGUUU 5'
hsa-miR-133a
Human SNX30 NM_001012994
(149) (1462)
SNX30 3'UTR
(7574)
5' UUCAAUUAACUUAAAGGACCAAU 3'
3' GUCGACCAACUUCCCCUGGUUU 5'
hsa-miR-133a
Human ANXA2 NM_001002857
(137)
(1055)
ANXA2 3'UTR
(1562)
5' TACAGTATGGTTGCCCCTATCCAAG 3'
3' GUCGACCAACUUCCCCUGGUUU 5'
hsa-miR-133a
D
f-luc
3'UTR binding site
miR-133a
miR-NC
Relative luciferase activity
SGMS2
UBA2
SNX30
ANXA2
E
LNA-NC
LNA-133a
H&E
SGMS2
F
Relative SGMS2 mRNA expression
LNA-NC
LNA-133a

Figure 6. The low expression levels of miR-133a target genes correlate with poor survival of osteosarcoma patients. (**A-D**) Kaplan-Meier survival curves of disease-free survival according to the expression levels of the miR-133a target genes including *SGMS2* (**A**), *UBA2* (**B**), *SNX30* (**C**), *ANXA2* (**D**) in 35 patient biopsy samples. The optimal cutoff points were determined by the Youden index under the receiver-operating characteristic (ROC) curve. The statistical significance of differences were determined by the log-rank test.

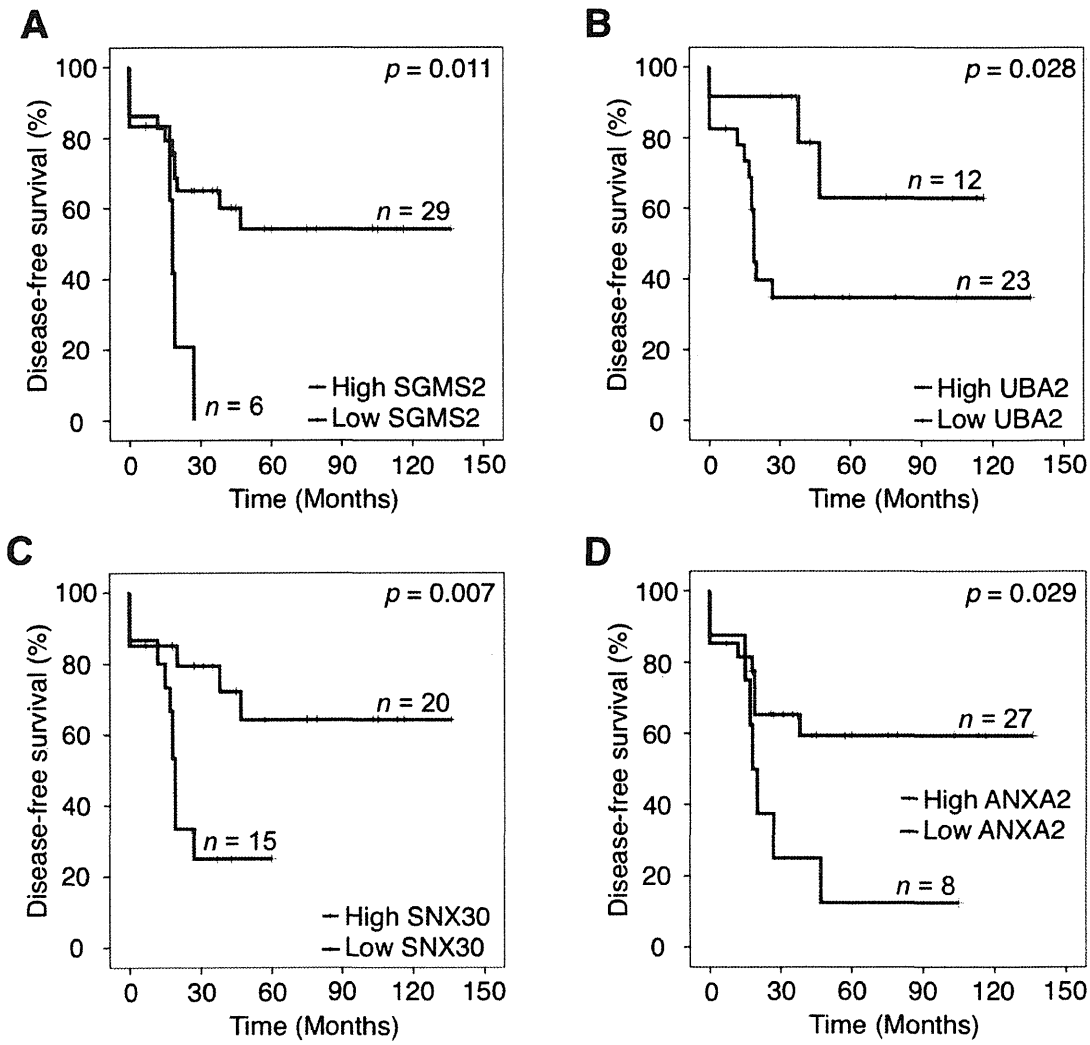

Advanced Drug Delivery Reviews 65 (2013) 376–382

Contents lists available at SciVerse ScienceDirect

Advanced Drug Delivery Reviews

journal homepage: www.elsevier.com/locate/addr

Exosomal tumor-suppressive microRNAs as novel cancer therapy☆ "Exocure" is another choice for cancer treatment

Nobuyoshi Kosaka [a,*], Fumitaka Takeshita [a], Yusuke Yoshioka [a,b,d], Keitaro Hagiwara [a,c], Takeshi Katsuda [a], Makiko Ono [a], Takahiro Ochiya [a]

[a] Division of Molecular and Cellular Medicine, National Cancer Center Research Institute, 5-1-1, Tsukiji, Chuo-ku, Tokyo 104-0045, Japan
[b] Integrative Bioscience and Biomedical Engineering, Graduate School of Science and Engineering, Waseda University, Tokyo 162-8480, Japan
[c] Department of Biological Information, Graduate School of Bioscience and Biotechnology, Tokyo Institute of Technology, Yokohama, Kanagawa 226-8501, Japan
[d] Research Fellow of the Japan Society for the Promotion of Science (JSPS), Japan

ARTICLE INFO

Article history:
Accepted 8 July 2012
Available online 25 July 2012

Keywords:
Tumor-suppressive microRNA
Secretory microRNAs
Cell–cell communication
Tumor initiation
Exosomes
Small RNA therapy
Drug delivery system
Exosome
Microvesicle

ABSTRACT

MicroRNAs (miRNAs) act to fine-tune cellular responses in a variety of biological circumstances such as development, organogenesis, and homeostasis. The dysregulation of miRNA expression accelerates disease progression, including metabolic disease, immunological disease and cancer, through the gene network disorder. Therefore, understanding the miRNA maturation process may unravel the mechanisms of cancer malignancy; however, the life of miRNA has not been clarified. In this article, we summarize the recent findings regarding the novel forms of miRNA, especially secretory miRNAs, focusing on exosomal miRNAs. Recent research has revealed that exosomal miRNAs affect many aspects of physiological and pathological conditions, and may be useful as novel therapy. Here, we propose a method for the delivery of tumor-suppressive miRNAs to desired sites using exosomes, and we named this method "exocure".

Contents

☆ This review is part of the *Advanced Drug Delivery Reviews* theme issue on "Exosomes: a key to delivering genetic materials".

* Corresponding author at: Division of Molecular and Cellular Medicine, National Cancer Center Research Institute, 1-1, Tsukiji, 5-chome, Chuo-ku, Tokyo 104-0045, Japan.
E-mail address: nkosaka@ncc.go.jp (N. Kosaka).

0169-409X/$ – see front matter © 2012 Elsevier B.V. All rights reserved.
doi:10.1016/j.addr.2012.07.011

1. Introduction

MicroRNAs (miRNAs) are small, non-coding RNAs that are approximately 22 nt in length [1]. Although more than 1500 mature human miRNA sequences are currently listed in the miRNA database [2], the function of many has not been clarified. The maturation process of miRNAs includes several post-transcriptional processing steps [1]. First, the primary miRNA transcripts (primary miRNAs; pri-miRNA) are generated from the genomic sequence. These long transcripts are mainly transcribed by RNA polymerase II. Second, these transcripts are processed to precursor miRNA (pre-miRNA) in 60–110 nt fragments in the nucleus by Drosha, an RNase III enzyme. Then the pre-miRNAs are transported to the cytoplasm by exportin-5. Dicer, another RNase III enzyme, processes the pre-miRNA into double-stranded RNA, which is a mature miRNA of approximately 22 bp. The mature miRNA is composed of an RNA-induced silencing complex (RISC) and binds to the complementary sequence in the 3′ untranslated region (3′ UTR) of target mRNAs, resulting in the degradation of the mRNA and/or inhibition of protein translation [3]. This multistep processing is regulated by many factors such as epigenetic modifications of the genomic sequence and by transcription factors, RNase and RNA-binding proteins. If there is a misregulation of one of these processing components, the miRNA expression will be dysregulated, leading to disease progression such as cancer malignancy [4]. Recently, it was reported that miRNAs do not exist only in the cell but are also secreted outside of cells [5,6]. In this review, we will discuss recent reports that indicate that exosomes carrying "secretory miRNAs" mediate various biological phenomena. In addition, we propose the usage of an exosome-delivered tumor-suppressive miRNA in cancer therapy.

2. Tumor-suppressive miRNAs are novel anti-cancer agents

It is known that the downregulation of miRNA expression leads to cancer development through various mechanisms such as genomic deletions, amplifications, mutations, epigenetic silencing, the dysregulation of transcription factors that target specific miRNAs, or the inappropriate processing of miRNA precursors [4]. These downregulated miRNAs are thought to act as tumor suppressors. There are various types of tumor-suppressive miRNAs; however, little is known regarding their precise mechanism of action (Table 1).

2.1. let-7

The expression of let-7 miRNA is significantly downregulated in lung cancer, and the overexpression of let-7 in a lung adenocarcinoma cell line suppressed lung cancer cell growth in vitro through the downregulation of KRAS and HMGA2 [7–10]. Interestingly, let-7 miRNA expression was markedly reduced in breast cancer tumor-initiating cells [11], which have self-renewal ability and resistance to chemotherapy and radiotherapy, and the expression of let-7 miRNA increased after differentiation [12]. The re-expression of let-7 in breast cancer tumor-initiating cells reduced proliferation, mammosphere formation and metastasis in a xenograft model through the reduction of KRAS and/or HMGA2. Many downregulation mechanisms of let-7 have been reported [13–19]. Importantly, disruption of the let-7 precursor processing by LIN28 and LIN28B, which are reported as overexpressed in primary human tumors, human cancer cell lines and pluripotent stem cells, is essential for controlling proper miRNA expression [14].

2.2. miR-16

MiR-15a and miR-16-1 are deleted or downregulated in the majority of chronic lymphocytic leukemia (CLL) cells [20–22], and re-expression of these miRNAs induced apoptosis through the downregulation of BCL2. In addition, the miR-15a and miR-16 levels significantly decrease in advanced prostate tumor cells [23]. Takeshita et al. reported that the injection of miR-16 with atelocollagen (a highly purified type I collagen that possesses low immunogenicity and is produced by treating calf dermis with pepsin) via the tail vein of mice significantly inhibited the growth of prostate bone metastases in a therapeutic bone-metastasis model [24].

2.3. miR-143

The suppression of miR-143 expression has been reported in several human cancers, including colorectal, prostate, cervical and ovarian [25–30]. Induction of miR-143 expression in those cancer cells resulted in the inhibition of cell proliferation or the induction of apoptosis through the suppression of its target genes such as KRAS and ERK5. Furthermore, Osaki et al. showed that miR-143 was the most downregulated miRNA in metastatic human osteosarcoma cell lines relative to the parental cell lines, and transfection of miR-143 into metastatic human osteosarcoma cell lines significantly decreased cell invasiveness but not proliferation [31]. In addition, intravenous injection into mice of miR-143 significantly suppressed the formation of lung metastases from metastatic human osteosarcoma cell lines. Moreover, cells positive for MMP13, a target of miR-143 in osteosarcoma cells, was found in lung metastasis-positive cases but not in at least three cases with higher miR-143 expression levels and without metastases.

2.4. miR-22

Xu et al. demonstrated that miR-22 expression is upregulated in senescent human fibroblasts and epithelial cells. In contrast, its expression is downregulated in various cancer cell lines, and the overexpression of miR-22 in those cases induces growth suppression

Table 1
The list of typical tumor suppressive miRNAs.

microRNA	Type of cancer	Target gene	Phenotype	References
let-7	Lung cancer	KRAS	Inhibition of cell proliferation	[7–19]
	Breast cancer	HMGA2		
miR-16	Chronic lymphocytic leukemia	BCL2	Induction of apoptosis	[20–24]
	Prostate cancer	CCND1	Inhibition of cell proliferation	
		WNT3A		
miR-143	Ovarian cancer			[25–31]
	Prostate cancer	ERK5	Induction of apoptosis	
	Cervical cancer	KRAS	Inhibition of metastasis	
	Osteosarcoma		Inhibition of cell proliferation	
miR-22	Colorectal cancer	Sp1		[32]
	Breast cancer	CDK6	Induction of growth suppression	
		SIRT1	Induction of senescent phenotype	

Representative cases are shown in the "type of cancer" and "target gene".